

EPJ E

Soft Matter and
Biological Physics

EPJ.org
your physics journal

Eur. Phys. J. E (2011) **34**: 94

DOI: 10.1140/epje/i2011-11094-7

The role of the dynamic crossover temperature and the arrest in glass-forming fluids

F. Mallamace, C. Corsaro, H.E. Stanley and S.-H. Chen



The role of the dynamic crossover temperature and the arrest in glass-forming fluids

F. Mallamace^{1,2,3,a}, C. Corsaro^{3,4}, H.E. Stanley², and S.-H. Chen¹

¹ Department of Nuclear Science and Engineering, Massachusetts Institute of Technology, Cambridge, MA 02139, USA

² Center for Polymer Studies and Department of Physics, Boston University, Boston, MA 02215, USA

³ Dipartimento di Fisica and CNISM, Università di Messina I-98166, Messina, Italy

⁴ Fondazione Fulvio Frisone, Via Etnea, Catania, Italy

Received 2 May 2011

Published online: 23 September 2011 – © EDP Sciences / Società Italiana di Fisica / Springer-Verlag 2011

Abstract. We discuss the role of the dynamic glass-forming fragile-to-strong crossover (FSC) in supercooled liquids. In the FSC, significant dynamic changes such as the decoupling (the violation of the Stokes–Einstein relation) of homologous transport parameters, *e.g.*, the density relaxation time τ and the viscosity η , occur at a characteristic temperature T_c . We study the FSC using a scaling law approach. In particular, we use both forms of the mode-coupling theory (MCT): the original (ideal) and the extended form, which explicitly describes energy hopping processes. We demonstrate that T_c plays the most important physical role in understanding dynamic arrest processes.

1 Introduction

Glass transition (GT) is the material component of dynamic arrest (jamming), a phenomenon of great interest across a wide range of scientific fields. GT occurs when the temperature is decreased or when some other thermodynamic variable, *e.g.*, density or pressure, is changed. Although much research has been done using sophisticated theoretical models and various experimental techniques, GT is far from being completely understood [1, 2].

A usual method of obtaining a GT is to rapidly quench the system through a transformation range to very low T . Below a given temperature T_g , an amorphous “glassy” material is produced. The phenomenon is also characterized by both hysteresis effects and a nonlinear response, terms that are not apt in characterizing a glass because a glass is strongly affected by the history of its production. Macroscopic size and rapid T variation of the system time scales are essential if the phenomenon is to appear at $\approx T_g$, and a full microscopic understanding of the corresponding relaxation process is needed if experiments in this region are to be evaluated. Note that T_g is an important quantity when experimentally characterizing the system.

Supercooled liquids, *i.e.*, liquids cooled below their melting point (T_M), are a good illustration of the basic mechanism of this intriguing phenomenon. In principle, all liquids may be supercooled. In some cases crystallization takes place in the proximity of T_M , in others the physical evolution of a liquid is still observable on further cooling,

and the liquid eventually solidifies directly into the glass phase. In this latter case, all the dynamic properties of the material can be observed as it is arrested as a frozen liquid. One example is the dramatic increase in the shear viscosity η that within a few degrees evolves from 10^{-2} to 10^{-1} poise, from typical values of a simple liquid in its normal state to values that exceed 10^{12} poise within the supercooled state—a remarkable dynamic slowing-down by more than 13 orders of magnitude [3, 4]. The viscosity, like any other transport coefficient—the average relaxation time τ_α and the self-diffusion coefficient D_s , reflects the underlying motion of the molecules in the system. Thus the time scale of the dynamics of supercooled liquids bridges the gap between microscopic and macroscopic times. These strongly T -dependent processes have been referred to as structural relaxation processes and are key in clarifying the physics of the GT process, and its basic microscopic origin in particular.

Glasses are non-equilibrium materials and, according to the experimental definition, are considered solids, *e.g.*, they are capable of sustaining static shear stresses. Compared to crystalline solids, however, they lack long-range order. In terms of transport parameters, a glass is solid only in the sense that the time scale used to characterize typical liquid-like flow phenomena τ becomes so large that it approaches infinity on normal experimental time scales. The flow phenomena, which demonstrate that a glass is not an ideal solid, manifest themselves as structural relaxation processes. This is the reason why the characterization of the latter is an important task in glass research.

^a e-mail: francesco.mallamace@unime.it

The central part of the liquid-to-glass transition problem concerns the question: how do the structural relaxation processes behave upon gradual cooling of the liquid?

Structural relaxation phenomena have been studied in great detail in recent decades through use of various theoretical models, dynamic simulations, and experimental approaches. Most of the studies focusing on dynamics examine motion through large temporal intervals of $10^{-12} < \tau < 10^2$ s, or even longer. Although this first seems to be the relevant dynamic window for exploring the transition from the supercooled viscous liquid to the glassy solid, within this window all the spectra of glass formers change gradually, and there is no way to meaningfully identify a liquid-to-glass transition temperature T_g . On examining the measured τ , η , and D_s data as a function of T , no anomalies that would indicate the presence of a liquid to glass crossover can be observed. The only characteristic property is that a form of diverging behavior is evident when T is decreased.

Although T_g is usually associated with specific heat, in terms of transport T_g is defined as the temperature at which the viscosity of the liquid is 10^{13} poise or when the relaxation time is 10^2 s. Although the calorimetric T_g refers to the transition from a strongly supercooled liquid to a glass, if we base our approach on generalized hydrodynamic equations [5–9], considering the specific heats $c_v = c_v(\omega)$ and $c_p = c_p(\omega)$ to be frequency dependent and generalizing the transport coefficients—which are also wave vector (q) dependent, *e.g.*, the heat conductivity $\lambda(q, \omega)$ —we see that T_g is located at the point where the relaxation times become macroscopic, *e.g.*, 10 s to 10^4 s. Specific-heat experiments are usually performed by monitoring the rate at which the energy E is added to or subtracted from the system ($\partial E/\partial T$) and measuring its temperature T as a function of the time t . When T is decreased, the supercooled glassing-liquid exhibits a jump ΔC at a certain temperature. In contrast, the curve for crystalline samples is smooth from the lowest temperatures at T_M . The location of the jump “defines” T_g . (Similar jumps occur in the thermal compressibility $\Delta\kappa$ and the expansivity $\Delta\alpha$.) This value of T_g and the behavior of $C(T)$ (ΔC , T_g and the T interval of the liquid/glass crossover) are strongly dependent not only on the scanning speed but also on the physical property measured.

The clarification of the underlying microscopic origin of this slowing-down is a hot topic of much current research. A common opinion is that the manner in which the dynamic quantities approach their limiting values reveals much about the nature of the arrest phenomenon. The observation that, as T decreases to a fraction of T_M , transport coefficients increase to several orders of magnitude, surpassing in many cases the time required for experimental accessibility, has been considered for long time the onset of a “diverging behavior”: a phase transition to a state in which the dynamic quantities become infinite following analogous laws of universality and scaling of critical phenomena. Although in the presence of conflicting opinions on the consistency of this approach in terms of “criticality” in the system properties [10–15], many theoretical models, molecular dynamics simulations, and refined experiments

have been conducted to understand dynamic arrest. Although these extensive studies have proposed many new ideas and possible interpretations of the arrest, essentially only a single mathematical form has been used over the years to treat the dynamic data of the glass forming materials: the Vogel-Fulcher-Tammann (VFT) equation.

On this basis, and understanding that transport parameters change gradually as a function of T , two relevant questions about dynamic arrest remain open:

- i) Is there a way to identify meaningfully a liquid-to-glass transition temperature? In terms of viscosity and relaxation times, there is no precise liquid-to-glass transition temperature, only a transformation region—and the resulting glass is just a high-viscosity supercooled liquid state. There is no distinction between the glassy and the supercooled liquid states.
- ii) Do the dynamic parameters of the glass-forming materials have a “diverging behavior,” *i.e.*, is the dynamic arrest characterized by a phase transition to a state in which the dynamic quantities become infinite following laws analogous to the universality and scaling of critical phenomena? Is there experimental evidence that a conventional phase transition is the origin of glass formation?

As a liquid approaches the glass phase it is not spatially homogeneous [16–19] and it exhibits so-called dynamic heterogeneities (DH). These are characterized by regions of space that exhibit strong dynamic correlations where transport parameters are decoupled so that the Stokes-Einstein (SE) relation is violated at a certain dynamic crossover temperature (T_\times) within a region T_g to T_M located inside the supercooled phase. For many years studies on glass-forming liquids have proposed that inside the region of the supercooled phase limited by T_\times transport parameters can have universal features [12, 20–25].

Our work seeks to demonstrate that the dynamic arrest process is essentially due to a dynamic crossover above the calorimetric T_g , at which point significant couplings in the system dynamics occur. This observation reveals a potentially intriguing picture of dynamic universality in which the crossover temperature is the main factor.

2 State of the art

The mode-coupling theory (MCT) in its ideal form focuses on the relation between collective density fluctuations and single molecule dynamics in a cage model [10]. Using the MCT in this context we see that the structural relaxations are characterized by a bimodal decay (a two-step relaxation scenario) in the time-dependent density correlation function. This is typically measured by means of light-scattering and neutron-scattering and dielectric relaxation frequency spectra—primary α - and secondary β -processes in which molecules explore all the available cage space. In the quasi-elastic-scattering time regime the two contributions are superimposed, with the β contribution at the lowest time (just above the microscopic contributions), but in the dielectric loss spectra frequency

regime such a contribution is located at a frequency above the α -peak frequency $\omega_\alpha = 1/\tau_\alpha$. In the β -process the relaxation times extracted by the dielectric spectra can be described using an activated Arrhenius T behavior $\ln \tau_\beta/\tau_{\beta 0} = E(T)/k_B T$, a behavior that differs significantly from a Super-Arrhenius (SA) or a Vogel-Fulcher-Tammann (VFT) behavior in which τ_α diverges. The main finding of the MCT is that the transport data (with two structural relaxation time scales) indicate the existence of a crossover temperature T_c located above T_g , at which the transport changes from one that is typical of a strongly coupled fluid to one that is characteristic of a glass. Near T_c , the α -relaxation—which governs the macroscopic time dynamics on the fluid side and is characterized by a power law divergence of the relaxation scale and the anomalies of the Debye-Waller factor—exhibits hierarchical multi-exponential temporal decay (the well-known stretched exponential form $F(q, t) = F_q^c \exp[-(t/\tau_\alpha)^\beta]$ [10]). In contrast, the β -process reveals the crossover approaching with two fractal time-decay behaviors (exhibiting non-universal exponents). Short times produce identical dynamics from both the fluid and glass sides, and long times produce correlation functions that saturate in the glass phase but decay algebraically in the fluid phase. The ideal MCT crossover temperature can be calculated from the two time scales and, in particular, for the α -process by means of a power law

$$\tau_\alpha = \tau_{\alpha 0} \left| \frac{T - T_c}{T_c} \right|^{-\gamma}, \quad (1)$$

where γ is a non-universal exponent. This latter form describes well the α -relaxation times obtained from dielectric experiments and the viscosity data of supercooled fluids when $T_M > T > T_c$, and thus the temperature region from the liquid stable phase to the coupled fluid phase, *i.e.*, the moderately supercooled state. This is a limit of the ideal MCT [10]. A very similar power law approach has been used, independent of the MCT, to describe the strong increase in transport parameters that occurs when the lowering temperature of a normal liquid enters the moderately supercooled region [7, 20–23]. This approach was used to investigate the dynamics of glass-forming liquids by the explicit inclusion of the cooperative nature of their transport processes on a microscopic scale [7, 26].

In recent decades, this slowing-down of transport—from the stable liquid phase to the deepest supercooled regime, including in many cases the calorimetric glass transition temperature T_g —has been described using the VTF equation,

$$\eta = \eta_0 \exp\left(\frac{B}{T - T_0}\right) = \eta_0 \exp\left(\frac{D_T T_0}{T - T_0}\right), \quad (2)$$

a form that accurately predicts diverging behavior at a non-zero temperature T_0 and a strength coefficient D_T related to the concept of “fragility.” The excellent data fit and its few parameters, together with the diverging scales (of $\tau(T)$, $D_s(T)$, and $\eta(T)$) contained within eq. (2) are essential ingredients when describing the arrest process

as an underlying phase transition to a state of infinite relaxation time [27]. Thus a large class of experiments have also used the VFT formalism to relate T_0 to the temperature T_g , *i.e.*, $T_M > T_g > T_0$.

In recent years this has been confirmed by associating the VFT fitting parameter T_0 with the Kauzmann temperature T_K [13], *i.e.*, $T_0 \sim T_K$. As an ideal glass temperature, T_K is defined as the temperature at which the configurational entropy S_C of the liquid phase extrapolated below the glass transition converges with the crystal phase entropy. This can be understood using the Adam-Gibbs theory [27] which relates the T -dependence of the structural relaxation time, τ_α , to the change in S_C , *i.e.*, $\tau_\alpha = \tau_0 \exp(C/T S_C)$. If S_C goes to zero at a finite temperature (*e.g.*, $S_C = a(T - T_K)/T$), then we obtain the VFT form when T_K is identified with T_0 . Indeed, this identification between T_K and T_0 supports the physical validity of eq. (2).

In describing the dynamics of supercooled liquids, Arrhenius behavior is when a single particle hops over barriers of uniform height, and the cooperative super-Arrhenius behavior is when the barriers have a broad distribution of heights. Super-Arrhenius behavior describes the thermodynamics of supercooled systems in terms of their so-called inherent structures [28, 29]. This approach utilizes potential energy topology, *e.g.*, the number and depth of local minima (basins) of the potential-energy landscape. Within this framework, the short-time dynamics of the supercooled liquid are characterized as intrabasin motion and the long-time slow dynamics as interbasin motion.

Glass-forming liquids have long been classified in terms of their “fragility” [3]. “Fragile” liquids have a marked VFT temperature dependence and “strong” liquids exhibit pure Arrhenius dynamic behavior. The Arrhenius distortion of different fluids on approaching the dynamical arrest is quantified in terms of their fragility D_T . Although VFT has often been treated as a “universal” feature of supercooled fluids, this has been questioned, *e.g.*, it has been pointed out [30] that $B = D_T T_0$ does not in fact yield the Arrhenius form for $T_0 = 0$.

In addition to the possible “criticality” of the arrest process, this classification of liquids as “fragile” or “strong” has given rise to two other relevant aspects of the dynamic arrest puzzle:

- i) It is possible that some supercooled liquids show a dynamic FSC at a certain temperature T_\times (where $T_g < T_\times < T_M$) [20], *i.e.*, there is a temperature that marks the boundary between two types of viscous behavior. The liquid viscous behavior is Arrhenius for $T_g < T < T_\times$ and super-Arrhenius for $T > T_\times$, and the corresponding data can be fit using a power law form similar to eq. (1). The existence of a FSC at $T_\times \sim 228$ K has been proposed for water [31]—in a manner similar to the proposal that such thermodynamical anomalies of water as the isothermal compressibility K_T exist—by assuming that the occurrence of the phenomenon corresponds to a change in the local structure of the liquid. Similar results have been obtained in a detailed comparison of DC con-

ductivity and dielectric relaxation of many different fluids, through the use of a temperature derivative approach [32].

- ii) Dynamical heterogeneities (DH) may be present. As mentioned above, this topic has recently received widespread attention [15, 18, 19, 33–36]. Due to microscopic cooperative processes, when a liquid approaches arrest there is an onset of high spatial correlations, *i.e.*, a rapid increase in characteristic length and time scales—a situation in which the α -relaxation time τ can depend on a typical length scale ξ , *e.g.*, $\tau = \exp(\mu\xi(T)/T)$. Thus, as T decreases in the supercooled region due to the molecular interaction, spatial regions appear in which the structural relaxation time differs by orders of magnitude from the average over the entire system. According to this description, the physics of the arrested process is dominated by so-called “spatially heterogeneous dynamics” [33]. It has been argued that the presence of these heterogeneities causes the breakdown of the Stokes-Einstein (SE) relation (or the appearance of the fractional Stokes-Einstein relation) and a dynamic FS crossover [17–19, 37] in a region located inside the supercooled phase at some temperature within the T_M – T_g range. Since the derivation of the SE relation assumes the uncorrelated motion of particles, it is reasonable that the onset of correlations could result in a failure of the same relation. If this is the case, the SE violation represents a useful approach to studying deeper aspects of the glass transition and other relevant phenomena observed in the T_M – T_g range.

The possible existence of a temperature T_x marking dynamical changes of fragile supercooled liquids below T_M has been already studied [12, 20–23, 38, 39]. This work assumes that the GT shows some degree of universality. Recently, the VFT dominance in describing the dynamics of glass-forming liquids has been questioned in terms of theory [15] and such alternative data analysis techniques as the Avramov form [24] $\tau(T) = \tau_0 \exp(B/T^n)$. In the first case, by considering a glass-forming system composed of particles interacting via soft potentials, it was explicitly demonstrated that the configurational entropy is finite at any temperature [15], *i.e.*, a Kauzmann temperature T_K , where the liquid is out of the equilibrium, does not exist and thus the VFT may be considered only a fitting form. In the second one, instead, the study [24] of the dielectric relaxation times $\tau(T)$ for 42 ultraviscous glass forming fluids confirms the previous suggestion that there is no compelling evidence for the VFT prediction that transport parameters diverge at a finite T providing a demonstration on the superiority, *versus* the VFT, of equations showing no divergence at a finite (non-zero) temperature (*e.g.*, Avramov); the validity of such scenario has been proved by considering the segmental relaxation data of glass-forming polymers as $T \rightarrow T_0$ [40]. Similar findings have been reported also for polymers and small molecule glass formers (see, *e.g.*, refs. [7–9] of ref. [40]), suggesting that the main finding of the model proposed for soft systems can be generalized.

Immediately following these studies, two additional approaches were proposed. The first approach, based on the parabolic form $[(T_o/T)]^2$, considers the relaxation times and the viscosities of 58 liquids and demonstrates that a certain degree of universality below the onset temperature T_o (defined as the temperature above which transport coefficients are T -independent) exists [25]. The second approach [41] applies a constraint theory to the Adam-Gibbs model basic equation ($\tau(T) = \tau_0 \exp(K/T \exp(C/T))$) and produces an improved description of the $\eta(T)$ and $\tau(T)$ of inorganic and organic materials with the same number of parameters as those of the previous equations. Very recently, by means of a distortion-sensitive enthalpy space linearized- or derivative-based empirical analysis, the validity of all these VFT alternative forms has been tested by considering the evolution of the primary α -relaxation time [42], demonstrating that the parabolic approach is less valid than the other approaches, and proposing the one associated with the Adam-Gibbs model to be the divergenceless successor to the VFT approach.

Over the course of studying glassy water by means of experimental [43–46] and molecular dynamic simulation [47–49] techniques in both confined and bulk supercooled contexts, we have observed that both the SE violation and the dynamic FS exhibit a crossover at the same temperature $T_x \sim 225$ K, with $T_g < T_x < T_M$. Drawing on these results we now use an extended MCT (EMCT) to study the general case of glassy materials [50, 51]. Note that although the ideal MCT assumes that structural relaxation is the bottleneck of all molecular motion, the EMCT, which includes density fluctuations, suggests that phonon-assisted hopping processes may explain structural relaxation processes [50].

We conclude that EMCT predicts a dynamic crossover in the τ_α and in D_s , as implied by the structure of its equations of motion. This crossover occurs near the critical temperature T_c of the idealized version of the theory, and is due to the change in the dynamics from the one determined by the cage effect to that dominated by hopping processes. When combined with a model for the hopping kernel developed from the dynamical theory for diffusion-jump processes, the crossover can be identified as a fragile-to-strong crossover (FSC) in which the α -relaxation time and the self-diffusion cross over from a non-Arrhenius to an Arrhenius behavior. Such a result, obtained for a Lennard-Jones system, provides a possible explanation of the FSC observed in a variety of glass-forming fluids. In addition, such an EMCT approach demonstrates that the Stokes-Einstein relation (SER) breaks down in different ways on the fragile and strong sides of the FSC, in agreement with the experimental observation in confined water. This study also demonstrates that the SER violation, in both the fragile and strong regions, can be fitted reasonably well by a single fractional relation with an empirical exponent of 0.85. For the self-diffusion coefficient, the EMCT gives $D_s \approx D^{\text{hop}} + D^{\text{id}}$, with the calculated values (see fig. 1, top) characterized by the dynamical crossover at $T \approx T_c$ from $D \approx D^{\text{id}}$ to D^{hop} . In particular fig. 1 shows the EMCT numerical results. The dashed curve refers to D^{id} , which must vanish at $T_c/T = 1$ with a

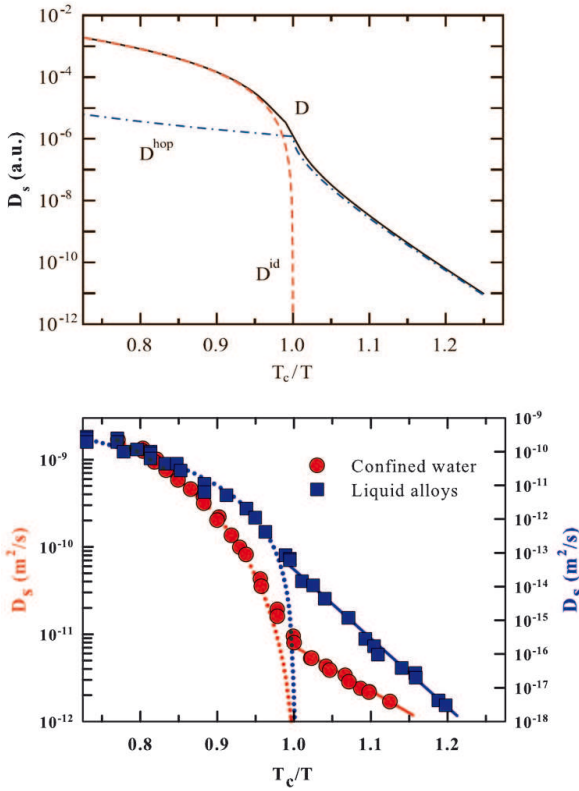


Fig. 1. The EMCT self-diffusion coefficient $D_s \approx D^{\text{hop}} + D^{\text{id}}$, with the calculated values (top panel) characterized by the dynamical crossover at $T \approx T_c$ from $D \approx D^{\text{id}}$ to D^{hop} . The dashed curve refers to the ideal contribution D^{id} that must vanish at $T_c/T = 1$ with a power law $D^{\text{id}} \sim |T - T_c|^\gamma$ according to the prediction of the idealized MCT, and the dashed-dotted curve represents D^{hop} due to the hopping processes. The bottom panel gives evidence of the full agreements between the EMCT results and the thermal behavior of glassing fluids by reporting the D_s data measured in two very different systems like confined water (NMR spectroscopy [45]) and liquid $\text{Pd}_{43}\text{Cu}_{27}\text{Ni}_{10}\text{P}_{20}$ alloys (radiotracers [52]); as can be seen in both cases, the MCT power law well fits the experimental data in the SA region indicating the temperature (T_c) where the experimental data cross toward a precise Arrhenius behavior.

power law $D^{\text{id}} \sim |T - T_c|^\gamma$ reflecting the dynamical arrest predicted by the idealized theory, and the dashed-dotted curve represents D^{hop} caused by the hopping processes. Again, the behavior of D_s from the EMCT is determined by the larger one between D^{hop} and D^{id} , and this explains why it crosses over from $D \approx D^{\text{id}}$ to D^{hop} near T_c . In addition, one infers from this figure that the self-diffusion coefficient exhibits nearly an Arrhenius behavior at low temperatures, hence the calculated EMCT D_s exhibits the FSC at $T \approx T_c$.

Such an EMCT analysis not only indicates the physical significance of the concept of T_c in terms of a well-established theory of glass-forming systems, but it also confirms all the water results: the FSC, and the break-

down of the SER both occurring near and below T_c , for which $T_\times \equiv T_c$. In addition, many features of dynamical heterogeneities emerge at this characteristic temperature and, in contrast, no singular physical characteristic are observed in the vicinity of the traditional glass transition temperature T_g [51]. To support the full agreement of the EMCT results and the thermal behavior of glassing fluids, at the bottom of fig. 1 we show the D_s data measured in two very different systems, *i.e.*, confined water (NMR spectroscopy [45]) and liquid $\text{Pd}_{43}\text{Cu}_{27}\text{Ni}_{10}\text{P}_{20}$ alloys (radiotracers [52]). Note that in both cases the MCT power law fits the experimental data in the SA region and indicates the temperature point ($T_\times \equiv T_c$) at which the experimental data cross that of the Arrhenius behavior.

3 Results and discussion

Using our EMCT findings, we conclude that the dynamic crossover temperature is a significant characteristic of dynamic arrest. After conducting an analysis of the data on 84 liquids [53], we believe this to be a significant universal feature, and that the T_c temperature—evaluated in terms of the MCT power law—is the most relevant for understanding the physics of dynamic arrest.

In fig. 2, four supercooled liquids: Glycerol [54], OTP [54], Salol [55], and bulk water [56] are shown. The $\eta(T)$ data are reported in an Arrhenius plot ($\log \eta$ vs. $1000/T$). Note that a crossover from a fragile-to-strong glass-forming behavior is evident in all the plots (except water) where the crossover temperature (T_c) is indicated by a star. The FSC is not observable in the water data because the system can be supercooled only within a limited T range. The measured T_c are located for the four materials in the supercooled liquid phase and are $T_c^{\text{GLY}} = 225 \pm 5$ K, $T_c^{\text{OTP}} = 274 \pm 5$ K, $T_c^{\text{SAL}} = 245 \pm 5$ K, and $T_c^{\text{H}_2\text{O}} = 225 \pm 5$ K for glycerol, OTP, Salol and water respectively. The data fits in all figures are shown by using three different functional forms: the Avramov (red curve), the parabolic (green curve), and the MCT power law (blue curve). Among these three, only the power law curve adequately reproduces the data points in all the SA region, and also predicts, for the reasons given above, the region within which the crossover temperature falls. The other forms only work within a limited T -range: the Avramov only at the highest T , and the parabolic in a finite range for $T > T_c$. In response to recent results concerning the non-diverging nature of supercooled materials [42, 57, 58], we have considered only those materials that are unambiguously characterized by a dynamical crossover without reporting a VFT data fit. The viscosity crossover temperature value obtained for salol agrees with the MCT analysis for the light scattering α and β relaxation times ($256 < T_c < 266$ K) measured in the same liquid [38, 39]. Finally, comparing the results among these four VFT alternative forms confirms the derivative test results of the α -relaxation time [42].

Figure 3 provides an additional test showing that many supercooled fluids are characterized by an Arrhenius behavior in the very-low-temperature region immediately

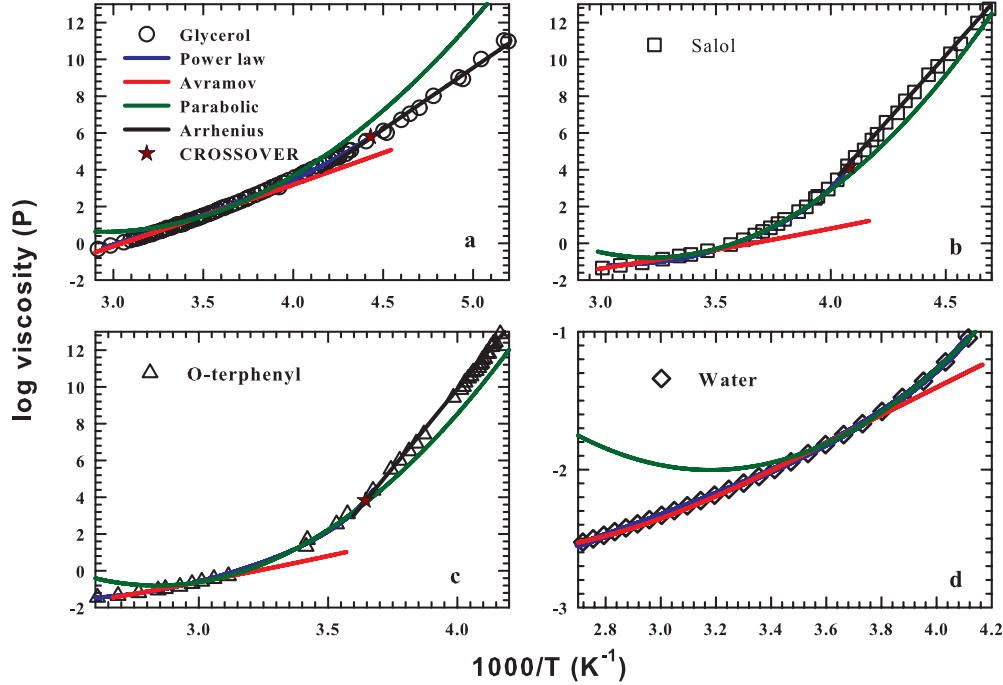


Fig. 2. (Colour online) The Arrhenius plot ($\log \eta$ vs. $1000/T$) of the viscosity of four well-known supercooled liquids: Glycerol [54], OTP [54], Salol [55] and bulk water [56]. As can be seen, a crossover from a fragile-to-strong glass-forming behavior is evident in all the plots (except water that can be supercooled only for a limited T range) where the crossover temperature (T_c) is indicated by a star. The measured T_c are located for the four materials in the supercooled liquid phase and are $T_c^{\text{GLY}} = 225 \pm 5$ K, $T_c^{\text{OTP}} = 274 \pm 5$ K, $T_c^{\text{SAL}} = 245 \pm 5$ K and $T_c^{\text{H}_2\text{O}} = 225 \pm 5$ K for glycerol, OTP, Salol and water, respectively. In all figures the data fitting, by using three different functional forms, are also reported: the Avramov (red curve), the parabolic (green curve) and the MCT power law (blue curve).

prior to dynamic arrest. This test assumes that the inverse temperature derivative of the logarithm of the transport parameters ($d \ln \eta / d(T^{-1})$ or $d \ln \tau / d(T^{-1})$) is constant if these quantities follow an Arrhenius behavior. At the lowest temperatures, the six fluids (Tri- α -naphthylbenzene, Salol, Dibutyl phthalate, B_2O_3 , α -phenyl-*o*-cresol, and *o*-terphenyl) are characterized by T -independent behavior of such quantities.

Taking into account the conclusions of ref. [24] and the suggestion [15] that the VFT approach should be reconsidered, we verified the universality of the FS crossover temperature in terms of an EMCT that considers the transport changes at the same temperature as the natural effects of the underlying system structure. In a temperature-dependent molecular structure, *i.e.*, a structure with characteristic local energy basins, the system particles exhibit two transition state trajectories: one in which $T > T_c$ and one in which $T < T_c$. According to the EMCT model, T_c can be the border temperature separating a region in which barrier effects are not important from a region in which they are essential, with the main factor being the hopping (Arrhenius) process. Thus, after properly fitting the transport quantities, for each liquid we evaluate the three parameters of the power law form: the significant T_c , the non-universal exponent γ , and the intercept value η_0

(or τ_0 and D_0). We are then able to construct a master curve that supports the validity of the MCT power law approach to describing the super Arrhenius temperature dependence of transport. The upper panel of fig. 4 is a plot of the viscosity in terms of $(\eta/\eta_0)^{-1/\gamma}$ vs. T/T_c . A single master curve is obtained. (We considered only 20 liquids, those for which a crossover is visually observable from the experimental data, although such an analysis has been successfully done on 80 supercooled fluids [53].) The lower panels show analogous master curves for self-diffusion (left, $(D_s D_0)^{1/\gamma}$ vs. T/T_c) and relaxation time (right, $(\tau/\tau_0)^{-1/\gamma}$ vs. T/T_c). The symbols identifying the fluid are the same as those in the viscosity case. Note that i) for the same liquid, within the error bars the T_c has the same value independent of the transport parameter used, and ii) the master curve, which is a scaled representation of eq. (1), is valid only for $T > T_c$, where the three master curves can be superimposed.

Figure 5 plots the viscosity $\eta(T)/\eta(T_c)$ vs. T_c/T of the 20 fluids normalized for crossover temperature. Two different behaviors above and below $(T_c/T) = 1$ are clearly evidenced. When $T < T_c$, the fluids have an Arrhenius behavior and, when $T > T_c$, they follow an MCT power law. The dotted lines represent the data fit of some fluids by means of eq. (1). When $T < T_c$ (the Arrhenius

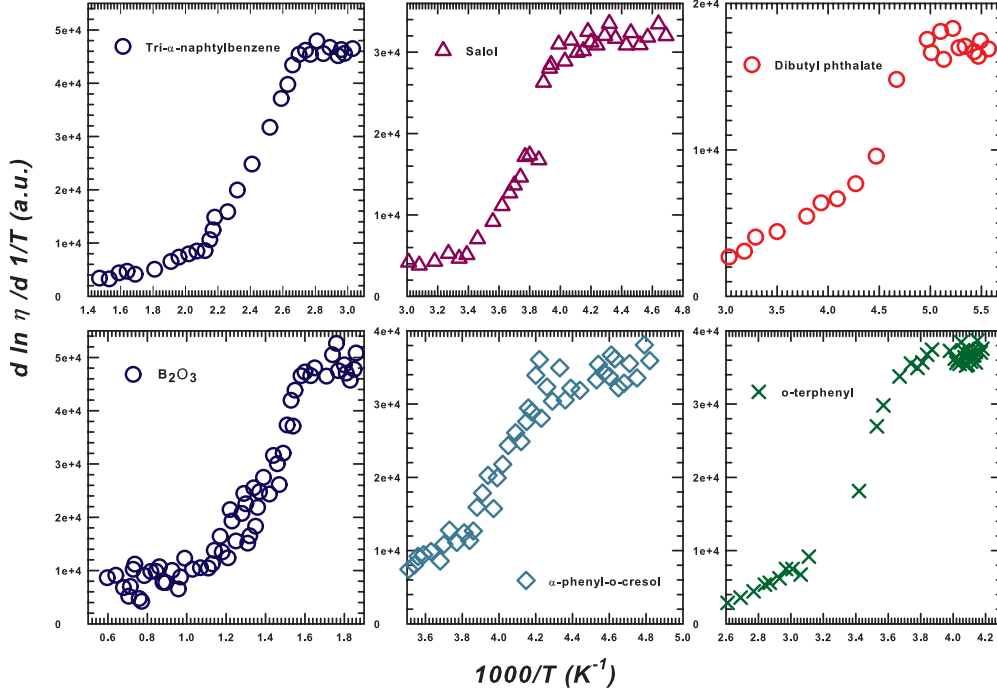


Fig. 3. The inverse temperature derivative of the logarithm of the viscosity ($d \ln \eta / d(T^{-1})$) of six supercooled fluids: Tri- α -naphthylbenzene, Salol, Dibutyl phthalate, B_2O_3 , α -phenyl- o -cresol and o -terphenyl. As can be seen, the lowest-temperature behavior is T -independent indicating an Arrhenius behavior just before the dynamical arrest.

side), the viscosity of the 20 reported supercooled liquids has a corresponding activation energy (E) that ranges from the high value of the polystyrene to the low value of germanium oxide, GeO_2 . This result agrees well with the EMCT approach, confirms the original suggestion that the transport processes are driven by hopping, and suggests that the crossover temperature T_c may be more significant in classifying the flow properties of liquids approaching a dynamic arrest temperature than the temperature T_0 of the VFT equation (*i.e.*, T_K) or the glass transition temperature T_g . In fact, many believe that the VFT is only a convenient fitting formula [15, 24, 41] and that there is no compelling evidence of any singular characteristic in the fluid transport properties around T_g . It appears instead that, when T decreases, the transport coefficients do not diverge but, on crossing T_c , alter their temperature dependence and resume an Arrhenius form.

If we evaluate the Debye-Stokes-Einstein ratio $R_{DSE} \equiv \eta / \tau T$ (see fig. 6 inset), or the Stokes-Einstein ratio $R_{SE} \equiv D_s \eta / T$, we observe a breakdown in R_{DSE} near T_c . This agrees well with an EMCT study [50] and other experimental observations of glass-forming liquids [18, 59–64] which indicate that these SE and DSE violations occur very close to T_c and are caused by a decoupling of transport coefficients [49] whose microscopic origins are due to dynamic heterogeneities at the onset of typical length scales that increase rapidly as T decreases [15]. To be

precise, although EMCT is able to predict the SE (and DSE) breakdown, the experiments reveal larger decouplings. This dynamic heterogeneity picture implies correlations between the time scale and the length scale: the increase in the time scale, as the arrest point is approached, leads to a growing length scale of dynamically correlated regions in space, suggesting that supercooled liquids may display dynamic scaling. Under these conditions and below a certain temperature the supercooling causes the SE (and the DSE) relations to give way to a fractional SE relation $D_s \sim \tau^{-\zeta}$, where the index ζ is related to the characteristic spatial-temporal length scales of the “spatially heterogeneous dynamics” [18, 59–64]. It has been proposed [14] that $\zeta = \alpha(T) / \beta(T)$ with α and β being temperature-dependent scaling exponents of D_s and τ , respectively. Analogous arguments hold for the viscosity η .

Figure 6 shows liquid transport parameters in terms of our scaling approach. For all the liquids we have proposed, the onset of the breakdown takes place at about the same value of viscosity, $\eta_x \sim 10^3$ poise, a value which is 8–10 decades lower than the value usually found near T_g . The principal result of this latter figure is the proposed universality degree. It is significant that this result emerges directly from the values of two transport parameters measured independently. The crossover temperature arises from a universal behavior rather than a definition linked to a specific cooling rate, such as the calorimetric

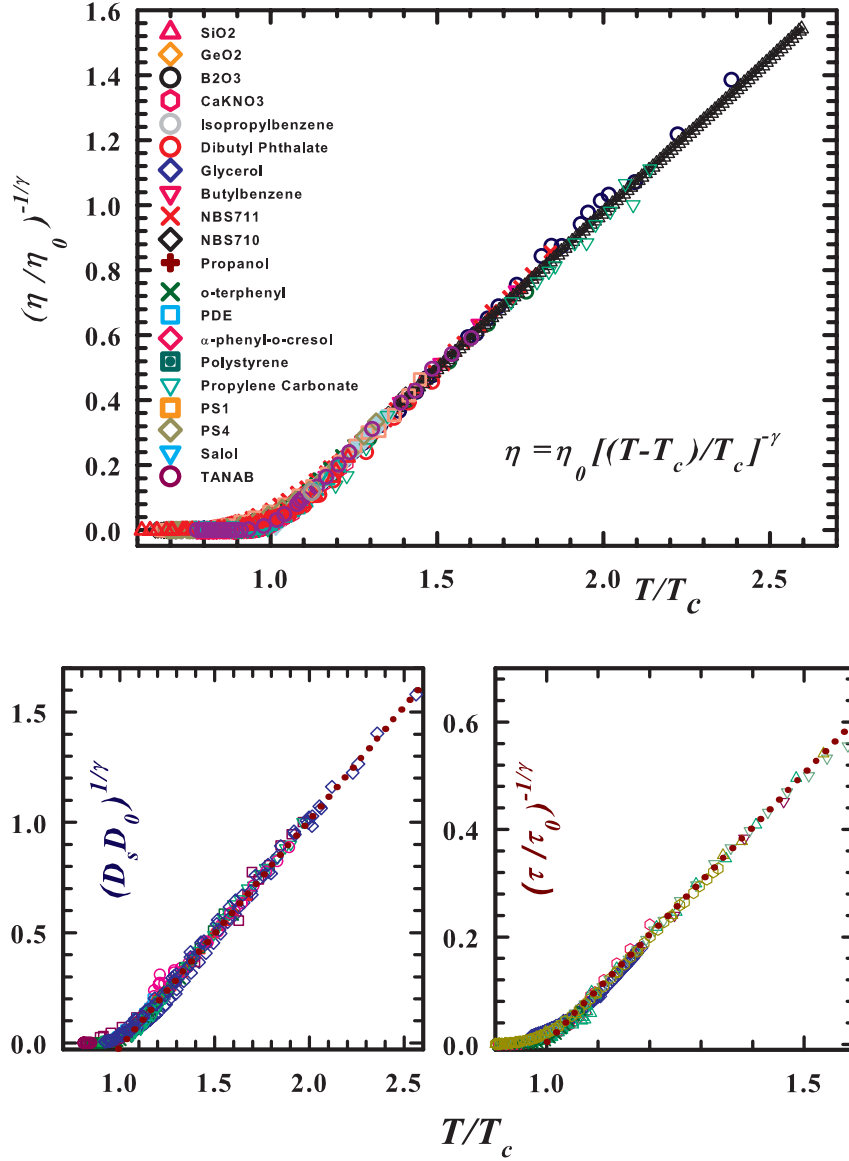


Fig. 4. Top panel: data collapse for the shear viscosity η for 20 indicated different liquids (including the 6 liquids of fig. 3, displaying Arrhenius behavior at the lowest T). Shown is the scaled viscosity $(\eta/\eta_0)^{-1/\gamma}$ as a function of the scaled temperature T/T_c . The non-universal scaling exponent γ takes on slightly different values for each liquid we studied, with $\gamma \approx 2 \pm 0.3$. Bottom panels show the self-diffusion constant D_s (left part), and the characteristic structural relaxation time τ (right part).

T_g . In the fractional DSE (and SE [53]), the decoupling in transport properties takes place at the crossover temperature T_c where the system recovers Arrhenius behavior.

The exponent of the DSE scaling plot is $\zeta = 0.85 \pm 0.02$ (approximately the same as that of the SE [53]). Figure 6 shows a correspondence at T_c among i) the dynamical FS crossover, ii) the breakdown of the Stokes-Einstein and the Debye-Stokes-Einstein relations, and iii) the dynamic heterogeneities. In addition, $\zeta = 0.85 \pm 0.02$ agrees with

experimental data [18, 45, 59, 62] and theoretical studies predicting a crossover from hierarchical SA dynamics for short length scales to pure Arrhenius dynamics at larger length scales as revealed by the EMCT approach (see the transport behavior shown in fig. 5). This crossover is caused by a change in the dynamics from those determined by the cage effect to those dominated by hopping processes [51].

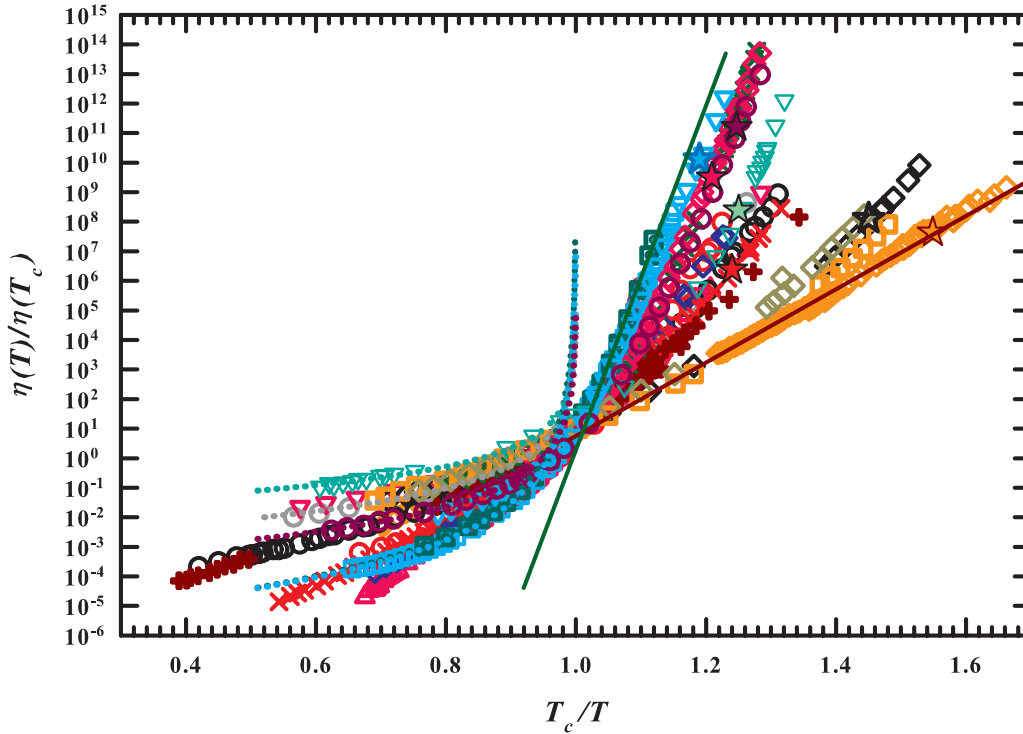


Fig. 5. The crossover temperature normalized representation, $\eta(T)/\eta(T_c)$ vs. T_c/T , of the viscosity for the 20 fluids considered. Two separate behaviors above and below $(T_c/T) = 1$ are clearly evidenced. For $T < T_c$ the fluids have a precise Arrhenius behavior whereas, in the opposite case they do follow the MCT power law (the dotted lines represent the data fitting of some fluids by means of eq. (1)). On the side where $T < T_c$, the Arrhenius activation energies (E) range from the high value of the polystyrene to the low one of germanium oxide, GeO_2 . Stars indicate the corresponding calorimetric T_g . This overall result agrees well with the EMCT approach, confirming the relevant indication that the crossover temperature T_c can be more significant for classifying the flow properties of liquids approaching the dynamical arrest.

4 Concluding remarks

As mentioned above, dynamic changes in SA glass-forming liquids have a structural origin. This can be clarified in terms of thermal fluctuations and corresponding density-density correlation lengths. A T decrease corresponds to a growth of correlated regions whose lengths can in principle diverge (like critical phenomena) causing the transport to slow down (*i.e.*, the invoked $\eta(T)$ divergence at a certain finite temperature). A phenomenon hampered by the dynamical crossover forcing this “apparent” criticality to evolve, at a certain temperature, towards a non-divergent behavior. The reason for this may be that in supercooled liquids this growth process originates solely in disordered and finite correlation regions (a kind of finite polydisperse dynamical clustering) whose molecules are more “sluggish” than those in the less correlated regions. The internal motions of these clusters are dynamic and strongly dependent on the temperature. A decrease in T causes them to progressively slow until they reach a temperature at which they are virtually frozen and an intercluster dynamic is the result. This is the crossover temperature, above it the molecular motion, identified by D_S and re-

flected in τ and η , depends on cluster dynamics. Cluster polydispersity and the interaction between clusters give rise to hierarchical relaxation times that are reflected in the time dependence of the density-density correlation function $F(q, t)$ as the well-known super-exponential decays and, in transport parameters such as η , as the super-Arrhenius behavior emerges.

These two dynamics have a different physical scenario. The first dynamic assumes the existence of a multibasin energy landscape (conceptually the same as the inherent structure entropy approach [28,29,65]) with a corresponding large frequency (and thus correlation time) distribution. The second dynamic assumes a two-state basin with a single frequency. At the highest temperatures the multibasin dynamic is favored, *i.e.*, the transport parameters exhibit super-Arrhenius behavior. Each of these basins is characterized by a temperature-dependent weight factor. When T decreases there is a progressive numerical reduction and the weight decreases to negligible values. At this stage the only relevant dynamic is the molecule migration from one cluster to another, *i.e.*, a hopping process with only one typical energy scale: the Arrhenius scale. In conclusion, the EMCT approach describes the situation well

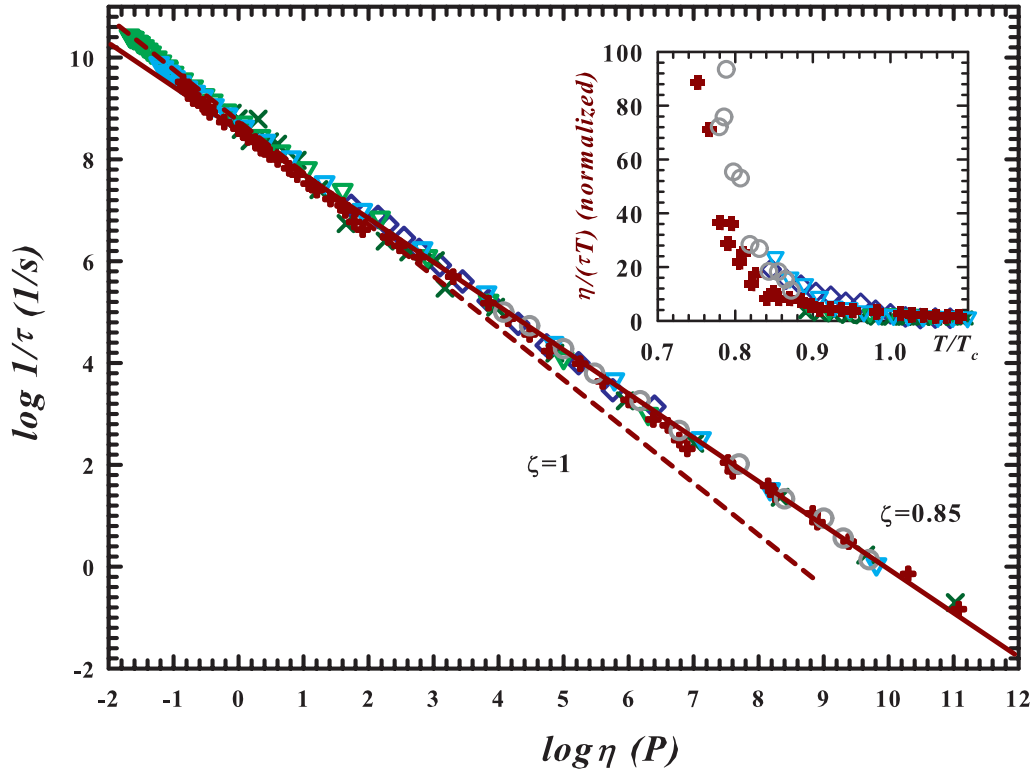


Fig. 6. The breakdown of the DSE law for 6 liquids that occurs just near the crossover temperature, identified by the MCT power law (inset). The main plot shows the *fractional* DSE, for all the liquids studied, the scaling exponent ζ takes almost the same value, $\zeta = 0.85 \pm 0.02$. We note that the onset of the DSE *fractional* breakdown takes place at about the same value of viscosity, $\eta(T_c) \approx 10^3$ poise. These data demonstrate a remarkable degree of universality in the temperature behavior of the transport properties of supercooled liquids confirming the special role of T_c to understand arrested processes.

by defining the dynamical crossover temperature to be one that reveals the two different dynamic regimes in terms of two different energy landscapes.

The data generated by EMCT, which incorporates barrier hopping caused by dynamic clustering reflected in energy landscapes, strongly support the idea that arrested processes may be characterized by a crossover in dynamic properties. We have seen that the singularity implied by genuine structural arrest is not supported by the existing experimental data, and that the VFT approach seems to lose any physical basis. Using a scaling law approach characterizing the MCT, we have analyzed the temperature dependence of the transport coefficients of many liquids and have demonstrated the existence of a well-defined fragile-to-strong dynamic crossover temperature T_c in the supercooled liquid regime. Note that the description of the transport in terms of MCT concepts confirms and explains the main finding of our previous analysis of 84 liquids: the dynamic crossover temperature is as important as the calorimetric glass transition temperature [53]. We have thus conclusively demonstrated that this phenomenon is a general property of all glass-forming liquids. Based on these considerations, we propose a different scenario for

dynamic arrest: as is shown in figs. 5 and 6, the main factor is the dynamic crossover. In particular, fig. 5 shows:

- i) that the FS crossover phenomenon can be more widely generalized than the traditional classification of liquids into two separate classes of glass formers, and
- ii) that transport coefficients only exhibit a significant change in behavior near T_c .

Previous classifications of supercooled fluids have been based on the assumption that the glass transition temperature T_g is phenomenologically defined as the temperature at which the viscosity of the liquid is 10^{13} poise (or when the relaxation time is 10^2 s). In our scaling law approach, the crossover MCT temperature separates two different dynamical regimes: the super-Arrhenius regime (far from the arrest point) and the Arrhenius regime (near the arrest point). This observation, based on results presented here, is fully supported by the current understanding of the MCT. Although the super-Arrhenius region can be described by its original formulation [10] (one that perhaps introduced the concept of the crossover temperature), the temperature behavior of the transport parameters seems to be better described using an extended form which incorporates barrier hopping [51].

Note that i) the FS crossover, the appearance of the fractional Stokes-Einstein violation, the Debye-Stokes-Einstein violation, and the dynamic heterogeneities are directly linked with T_c , and ii) the onset of the breakdown takes place at approximately the same value which is many decades lower than the value generally found near T_g .

Our conclusion is that a) T_c appears to be more relevant than T_g or T_0 to the physics of dynamic arrest phenomena, and b) the universality shown in the master curves from the scaled description of the Stokes-Einstein and Debye-Stokes-Einstein violations is a “ground-breaking” reality that suggests a new approach to exploring arrested processes. In this context, using the system concentration as the order parameter rather than the temperature might be a productive future approach to the study of dynamic arrest. Such a study would shed more light on dynamic arrest by approaching it from another direction and by utilizing the vast previous research on colloids and polymers and its technique of interpreting the evolution of transport parameters as a function of concentration.

The research in Messina is supported by the PRA-Unime-2008 and PRIN2008. The research at MIT is supported by DOE Grants DE-FG02-90ER45429 and 2113-MIT-DOE-591. The work utilized facilities of the Messina SCM-HR-NMR Center of CNR-INFN. HES thanks the NSF Chemistry Division (grant CHE-0911389 and CHE-0908218) for support. This work utilized facilities supported in part by the National Science Foundation under Agreement No. DMR-0086210.

References

1. P.W. Anderson, *Science* **267**, 1615 (1995).
2. K. Binder, W. Kob *Glassy, Materials and Disordered Solids: An Introduction to their Statistical Mechanics* (World Scientific, Singapore, 2005).
3. C.A. Angell, *Science* **267**, 1924 (1995).
4. J.C. Dyre, *Rev. Mod. Phys.* **78**, 953 (2006).
5. O.N. Birge, S.R. Nagele, *Phys. Rev. Lett.* **54**, 2674 (1985).
6. L.P. Kadanoff, P.C. Martin, *Ann. Phys. (N.Y.)* **24**, 419 (1963).
7. U. Bengtzelius, W. Götze, A. Sjölander, *J. Phys. C* **17**, 5915 (1984).
8. W. Götze, A. Latz, *J. Phys.: Condens. Matter* **1**, 4169 (1989).
9. J. Jäckle, *Physica A* **126**, 377 (1990).
10. W. Götze, L. Sjögren, *Rep. Prog. Phys.* **55**, 241 (1992).
11. V. Lubchenko, P.G. Wolynes, *Annu. Rev. Phys. Chem.* **58**, 235 (2007).
12. D. Kivelson, G. Tarjus, X. Zhao, S. Kivelson, *Phys. Rev. E* **53**, 751 (1996).
13. F.H. Stillinger, *J. Chem. Phys.* **88**, 7818 (1988).
14. J.P. Garrahan, D. Chandler, *Proc. Natl. Acad. Sci. U.S.A.* **100**, 9710 (2003).
15. J.P. Eckmann, I. Procaccia, *Phys. Rev. E* **78**, 011503 (2008).
16. U. Tracht *et al.*, *Phys. Rev. Lett.* **81**, 2727 (1998).
17. G. Tarjus, D. Kivelson, *J. Chem. Phys.* **103**, 3071 (1995).
18. J. Chang, H. Sillescu, *J. Phys. Chem. B* **101**, 8794 (1997).
19. M.D. Ediger, *Annu. Rev. Phys. Chem.* **51**, 99 (2000).
20. P. Taborek, R.N. Kleinman, D.J. Bishop, *Phys. Rev. B* **34**, 1835 (1986).
21. R. Richert, H. Bässler, *J. Phys.: Condens. Matter* **2**, 2273 (1990).
22. E. Rössler, *Ber. Bunsenges. Phys. Chem.* **94**, 225 (1990).
23. E. Rössler, K.U. Hess, V.N. Novikov, *J. Non-Cryst. Solids* **223**, 207 (1998).
24. T. Hecksher *et al.*, *Nat. Phys.* **4**, 737 (2008).
25. Y.S. Elmatad, D. Chandler, J.P. Garrahan, *J. Phys. Chem. B* **113**, 5563 (2009).
26. T.R. Kirkpatrick, *Phys. Rev. A* **31**, 939 (1985).
27. G. Adams, J.H. Gibbs, *J. Chem. Phys.* **43**, 139 (1965).
28. F.H. Stillinger, T.A. Weber, *Phys. Rev. A* **25**, 978 (1982).
29. F.H. Stillinger, T.A. Weber, *Science* **225**, 983 (1984).
30. G.P. Johari, *Philos. Mag.* **86**, 1567 (2006).
31. K. Ito, C.T. Moynihan, C.A. Angell, *Nature* **398**, 492 (1999).
32. F. Stickel, E.W. Fisher, R. Richert, *J. Chem. Phys.* **102**, 6251 (1995).
33. A.C. Pan, J.P. Garrahan, D. Chandler, *Phys. Rev. E* **72**, 041106 (2005).
34. J.D. Stevenson, J. Schmalian, P.G. Wolynes, *Nat. Phys.* **2**, 268 (2006).
35. E. Lerner, I. Procaccia, I. Regev, *Phys. Rev. E* **79**, 031501 (2009).
36. E. Lerner, I. Procaccia, J. Zylberg, *Phys. Rev. Lett.* **102**, 125701 (2009).
37. Y.J. Jung, J.P. Garrahan, D. Chandler, *Phys. Rev. E* **69**, 061205 (2004).
38. G. Li, W.M. Du, A. Sakai, H.Z. Cummins, *Phys. Rev. A* **46**, 3343 (1992).
39. Y. Yang, K.A. Nelson, *J. Chem. Phys.* **103**, 7732 (1995).
40. G.B. McKenna, *Nat. Phys.* **4**, 673 (2008).
41. J.C. Mauro *et al.*, *Proc. Natl. Acad. Sci. U.S.A.* **106**, 19780 (2009).
42. J.C. Martinez Garcia, J.L.I. Tamarit, S.J. Rzoska, *J. Chem. Phys.* **134**, 024521 (2011).
43. L. Liu *et al.*, *Phys. Rev. Lett.* **95**, 117802 (2005).
44. F. Mallamace *et al.*, *J. Chem. Phys.* **124**, 161102 (2006).
45. S.H. Chen *et al.*, *Proc. Natl. Acad. Sci. U.S.A.* **103**, 12974 (2006).
46. F. Mallamace *et al.*, *Proc. Natl. Acad. Sci. U.S.A.* **105**, 12725 (2008).
47. P. Kumar *et al.*, *Phys. Rev. Lett.* **97**, 177802 (2006).
48. P. Kumar *et al.*, *Proc. Natl. Acad. Sci. U.S.A.* **104**, 9575 (2007).
49. L. Xu *et al.*, *Nat. Phys.* **5**, 565 (2009).
50. S.H. Chong, *Phys. Rev. E* **78**, 041501 (2008).
51. S.H. Chong, S.H. Chen, F. Mallamace, *J. Phys.: Condens. Matter* **21**, 504101 (2009).
52. A. Bartsch, K. Rätzke, A. Meyer, F. Faupel, *Phys. Rev. Lett.* **104**, 195901 (2010).
53. F. Mallamace *et al.*, *Proc. Natl. Acad. Sci. U.S.A.* **107**, 22457 (2010).
54. K. Schroter, E. Donth, *J. Chem. Phys.* **113**, 9101 (2000).
55. W.T. Laughlin, D.R. Uhlmann, *J. Phys. Chem.* **78**, 2317 (1972).
56. C.H. Cho, J. Urquidi, S. Singh, G. Wilse Robinson, *J. Phys. Chem B* **103**, 1991 (1999).
57. L. Larini, A. Ottochian, C. De Michele, D. Leporini, *Nat. Phys.* **4**, 42 (2008).

58. A. Ottochian, C. De Michele, D. Leporini, J. Chem. Phys. **131**, 224517 (2009).
59. S.F. Swallen, P.A. Bonvallet, R.J. McMahon, M.D. Ediger, Phys. Rev. Lett. **90**, 015901 (2003).
60. J.F. Douglas, D. Leporini, J. Non-Cryst. Solids **235**, 137 (1998).
61. F. Fernandez-Alonso *et al.*, Phys. Rev. Lett. **98**, 077801 (2007).
62. M.K. Mapes, S.F. Swallen, M.D. Ediger, J. Phys. Chem. B **100**, 507 (2006).
63. L. Andreozzi, A. Di Schino, M. Giordano, D. Leporini, Europhys. Lett. **38**, 669 (1997).
64. D. Banerjee, S.N. Bhat, S.V. Bhat, D. Leporini, Proc. Natl. Acad. Sci. U.S.A. **106**, 11448 (2009).
65. S. Sastry, P.G. Debenedetti, S.H. Stillinger, Nature **393**, 554 (1998).